Implementing a New Snow Scheme in Simplified Simple Biosphere Model[①]

Sun Shufen (孙菽芬)

LASG, Institute of Atmospheric Physics, Chinese Academy of Sciences, Beijing 100029

Xue Yongkang (薛永康)

Department of Geography, University of Maryland, MD 20742, *USA*

ABSTRACT

This paper describes a modified version of SSIB through implementing a new snow model (SAST) in Simplified Simple Biosphere Model SSIB for climate study and presents the evaluation results by testing the scheme based on the field data from Russia and France. The relevant equations in the scheme are given, which describe complicated interactive processes among air–vegetation–snow–soil continuum through mass and heat exchange. An efficient numerical scheme is developed to solve the nonlinear equations successfully. By using the field data from Russia and France, the function of the new scheme is evaluated. The numerical results from the scheme show good agreement with field data. It indicates that the scheme developed here is workable and can be extended for climate study.

Key words: Snow cover model (SAST), SSIB, Implementing, Evaluation

1. Introduction

Over fifty percent land surface of the Northern Hemisphere can be seasonally covered by snow leading to significant spatial and temporal fluctuations in surface conditions. The properties of high albedo, lower thermal conductivity and low roughness length give rise to the impact from the micrometeorological scale (Kukla, 1981) to the global scale (Vernekar et al., 1995). It has been recognized that snow cover is also an active agent of climate variability over a variety of time scales (e.g., Walsh et al., 1985). Many modeling studies have been conducted to investigate snow processes and the interactions between atmospheric circulation and snow cover (e.g. Williams, 1975; Barnett et al., 1989; Cohen and Rind, 1991). From hydrological point of view, melted snow water represents an effective source of moisture for the soil and the timing of snow cover leads to a temporal shift in the runoff from hours to days up to a seasonal shift, especially melted period shift of deep snow cover towards to a period with intensive rain could give rise to heavy flood. Since snow cover strongly affects both global hydrological cycle and atmospheric processes, there is a need for reliable snow cover models in a wide range of fields, which can give accurate prediction of snow duration and extent, snow surface conditions such as albedo and surface temperature and its interactions with atmospheric and hydrological components. Furthermore, in areas with rare observational

database, snow cover models can be the useful tools for interpreting satellite pictures, traditionally problematic due to the similar radiation properties of clouds and snow cover in most wavelengths.

Despite the obvious importance of snow cover in climate studies, the description of snow processes is simple in many current and sophisticated land surface models. The parameterizations of snow processes used in current land surface models (LSMs) range greatly in terms of complexity. At the simple extreme, the model used by Manabe represents snow as a single layer with a prescribed albedo. Less complexity can be found in BASE's snow sub–model (Slater et al., 1998), which considers the effect of snow compaction but with a one layer scheme. Many sensitivity studies have shown that the models with one or two layers or very simple parameterizations of snow processes may not be able to give correct prediction. At the other extreme, the models with greater complexity are available (Anderson, 1976; Jordan, 1991) but these are numerically too time consuming to use in current GCMs. In between intermediate complexity, multi–layer scheme (could be more than three layers snow pack) such as those of Loth et al. (1992) and Lynch–Stieglitz (1994) include advanced albedo calculation based on snow age or temperature and explicitly model snow compaction, snow grain change, melted water drainage and others. SAST model (Sun et al., 1999) is one of intermediate complex models. It is based on the earlier developed complex and physically based snow models but with several major simplifications and improvements. SAST minimizes the number of snow layers as possible to no more than three layers, and has shown greater potential to capture important physical processes occurring in snow pack and predict relevant variables important to climate and hydrological study such as snow temperature, turbulent heat fluxes, runoff from snow melted water and snow duration timing.

All the above models with different comlexity, except for BASE's snow sub–model, are developed only to take the interactions among atmosphere–snow –soil continuum into consideration. They do not consider the effect of vegetation masking over snow cover and vice versa. On the other hand, even in many current sophisticated LSMs used in GCMs such as SSIB and BATS, there is only a simple interactive scheme between vegetation above and snow cover below, and the parameterizations of snow sub–model are too simple to capture some very important processes relative to climate study. They take snow mass balance into consideration with one layer model and constant snow density, and do not distinguish the thermal regime of snow from that of soil. In the real world, however, snow cover co–exists with vegetation canopy very often. So it is a critical and necessary step to implement an efficient and intermediately complicated sub–snow model in currently used LSMs. It is just the target of this work to implement SAST in SSIB. However, when a physically–based model like SAST is going to be implemented in a current land surface model like SSIB, there is a lot of work to do in order to bring interactive dependencies in the complicated atmosphere–vegetation–snow–soil continuum into line. In this paper, detailed description is given which explains how to bring SAST and SSIB models together into a new modified version of the SSIB for climate study. In Section 2, the governing equations in the new scheme are presented in detail first. In Section 3, the implicit combined difference equations are derived, which describe the interactive processes at the interfaces between vegetation masking and snow cover, and then an efficient numerical scheme for solving the highly nonlinear interactive equations is discussed. In Section 4, the numerical experiments for evaluating the scheme by using the field data in France and Russia are conducted and the numerical results comparing with field observational data are described.

2. The scheme of implementing SAST in SSIB

SAST presents a snow cover model and originally deals with atmosphere—snow—soil continuum only. There is no direct interaction between vegetation and snow cover in the original SAST. The snow model is at most three layers model (henceforth three layers model for simplicity) and predicts three temperatures, $T(z)$, and three snow water equivalent, w_j, for the three layers. There are two interactive interfaces on or under the snow pack: top interface between snow surface layer and atmosphere above and low interface between snow bottom layer and soil surface below. Thus the model needs to deal with energy and water exchange at the two interfaces: the latent and sensible heat fluxes at the top interface and the thermal heat flux and melted water infiltration flux (and runoff) at the low interface. First two fluxes at the top interface depend on the snow surface layer temperature and atmospheric temperature, and second two fluxes at the low interface depend on the temperatures of snow bottom layer and soil surface layer, and melted water flow behavior and soil physical properties. The soil zone, as a separate component with snow cover, receives the thermal heat flux and infiltration flux from snow body and changes its temperature vertically and moisture distribution independently. Besides, SAST also considers snow compaction process, and the snow density and snow depth, Z_t, change with time.

When there exists a snow cover under vegetation, SSIB uses a very simple adjustment scheme to 'Incorporate the Effects of Snow into the Simple Biosphere (SIB) Model' (discussed in Section 2.2 and Sellers et al., 1986): 1) As for energy balance aspect, the simple adjustment scheme in SSIB views the snow cover and soil body as an entirety but with some adjustments for thermal properties and does not distinguish the thermal regime of snow from soil. So, the simple adjustment scheme, same as in original SSIB with no snow cover existence, still uses one ground surface temperature, T_{gs}, and one average ground temperature, T_d, to describe the thermal behavior of the entirety. The latent and sensible fluxes at the interface between the surface of the entirety of snow, soil and air within canopy are dependent on the temperature of air within canopy and the temperature of the entirety surface. There is no interface between snow bottom and soil surface and thus there is no need to obtain heat flux at absent interface; 2) For snow cover mass aspect, the scheme assumes the snow density as a constant and records the snow mass accumulation variation (which considers the effects of snow falling and dry snow melted) over soil body in unit area, and thus the snow depth, Z_f, intercepted by the ground is equal to five times of the snow mass accumulation. Melted snow water is partitioned into soil moisture and runoff. Soil zone absorbs part of the melted water and adjusts its vertical moisture distribution; 3) To account for the effect of burying of vegetation by the snow accumulation on the turbulent transfer coefficients, the simple scheme defines a simple scale height h_f to estimate several adjusted parameters such as $\tilde{d}, \tilde{z}_0, \tilde{C}_1, \tilde{C}_2$ and $\tilde{S}_c$.

When SAST is implemented in SSIB, the snow cover with three layers scheme is sandwiched between vegetation above and soil body below, and the entire new structure will be quite different from either SSIB or SAST. Figure 1 schematically shows the interactive relations between different components being predicted in the new structure. In the figure, the snow cover is ranged between two waving lines. Comparing Fig. 1 with Fig. 3 in SSIB model with snow cover existence (Xue et al., 1991), it could be pointed out that

1) Since the entirety of snow cover and soil zone considered in SSIB is replaced by two separate components (snow cover with three layers and soil body below) in the new scheme, the physical space from the ground surface to air above canopy in SSIB is now replaced

by the physical space from the snow surface to air above canopy in the new scheme, and the lower boundary of the physical space changes from the ground surface in SSIB to the snow surface in the new scheme. It will introduce several corrections in the new scheme as follows. First, as mentioned before, it is necessary to account for the effect of burying of vegetation by accumulation snow on the turbulent transfer coefficients. The simple way in SSIB by defining a simple scale height h_f (as a function of snow depth, Z_f) to estimate several adjusted parameters such as $\tilde{d}$, $\tilde{z}_0$, $\tilde{C}_1$, $\tilde{C}_2$ and $\tilde{S}_c$ will be exactly followed in the new scheme but the function of the snow depth Z_f in SSIB should be replaced by the function of the snow depth Z_t. Second, when considering the transfer of solar radiation within canopy, lower boundary conditions such as albedo and surface temperature, T_{gs}, at the ground surface in SSIB are required. Since the ground surface is now replaced by the surface of snow top layer, the value of albedo and surface temperature at the ground surface in SSIB should be replaced by that of albedo, α_t, and surface temperature, $T(3)$ of the snow top layer in the new scheme. Third, when the sensible heat, latent heat and wind profile from the ground surface to air within canopy and from air within canopy to the air above canopy and relevant parameters such as resistance of r_b, r_d and others are considered in SSIB, the lower boundary conditions at the ground surface such as temperature and others are required again. Since the methods (including equations) to estimate the heat fluxes, wind profile and relevant parameters from the snow surface to the air within canopy and then to the air above canopy in the new scheme completely follow those in SSIB, it is obvious that the same lower boundary conditions are also required but should be defined at the surface of the snow top layer. And last, all the forcing conditions originally at the ground surface in SSIB, such as solar radiation and the effective precipitation (rain and / or snow) $P_0 = P - P_c + D_c$ after canopy interception and drainage, should become the forcing conditions on snow surface in the new scheme.

2) For thermal regime, the snow cover with soil zone below in SSIB is considered as the entirety but the snow cover in the new scheme is not combined with soil zone and both are considered as two seperate components. So, in the new scheme, there is a clear interface between snow bottom and soil surface below and it is necessary to determine the heat flux at the interface. But, there is no such interface and therefore there is no need to define the heat flux at the nonexistent interface between snow body and soil surface in SSIB. As for mass balance, both SSIB and the new scheme consider the processes of infiltration into soil zone and runoff from melted snow water. Of course, the scheme to quantify the processes in the new scheme is quite different from that in SSIB.

Finally, it should be pointed out that since the ground surface under vegetation is not so flat and smooth, the thin snow cover could be embedded in the concave surface of ground and its thermal properties such as temperature being not distinctly separated with ground surface. In this case, a simple switch is set up, i.e., the new scheme is operated only after snow cover depth exceeds some thickness (in the new scheme, the thickness is equal to 5 cm, however, this thickness should be fixed based on available data) and otherwise the new scheme will not be used and original SSIB will function again.

This section is devoted to the development of new scheme by modifying and combining the equations in SSIB and SAST. In order to be more consistent with SSIB and SAST models, we try to use original formulation and notation defined in SSIB and SAST models as much as possible (Xue et al., 1991; Sellers et al., 1986; Sun et al., 1999). In the new scheme, besides the equations defining energy budget and mass budget like in SSIB, there is one more equation of

snow compaction used in SAST to define snow density and snow depth. Next, we first give the equations in the order of vegetation; second, snow cover and the last soil body because it represents the vertical order of their existence in nature and also indicates the corresponding interaction relations one by one. In order to present the equation system more concisely, the meaning of all notations is listed in APPENDIX for reference.

2.1 *Governing equation of energy budget*

Canopy temperature

$$C_c \frac{\partial T_c}{\partial t} = Rn_c - H_c - \lambda E_c, \tag{1}$$

Enthalpy of snow layers (for at most three layers)

$$\frac{\partial H(z)}{\partial t} = \frac{\partial}{\partial Z}(- G_{sn}(z) - SH_{sn}(z)), \tag{2}$$

$$H(z) = C_V \times (T(z) - 273.16) - f_i \times L_{li} \times w_j \times \rho_w, \tag{3}$$

where

$$SH_{sn}(z) = SH_{sn}(z_3) \times \exp(- \kappa Z), \tag{4}$$

$$SH_{sn}(z_3) = SH_{sn}^* \times (1 - \alpha), \tag{5}$$

$$G_{sn}(z_3) = R_{sn,L} + G_{pr} - H_{sn} - \lambda E_{sn}, \text{ at the snow surface.} \tag{6}$$

$$G_{sn}(z) = - K(z)\frac{\partial T(z)}{\partial Z}, \text{ within the snow body.} \tag{7}$$

Ground surface temperature

$$C_{gs} \frac{\partial T_{gs}}{\partial t} = G_{gs} - \frac{2\pi C_{gs}}{\tau}(T_{gs} - T_d), \tag{8}$$

where $G_{gs} = G_{sn}(Z_0)$ at the snow bottom. $\tag{9}$

Soil deep layer temperature

$$C_d \frac{\partial T_d}{\partial t} = 2\pi C_{gs}(T_{gs} - T_d) / (\tau\sqrt{365\pi}), \tag{10}$$

where Rn_c, SH_{sn}^*, $R_{sn,L}$, are obtained using the same method in SSIB model, and the fluxes, H_c, H_{sn}, λE_c, λE_{sn} and G_{pr} are the functions of the atmospheric conditions, predicted variables and various resistances, and are given by

$$H_c = (T_c - T_a)\rho c_p / \bar{r}_b / 2), \tag{11}$$

$$H_{sn} = (T(3) - T_a)\rho c_p / r_d, (T(3): \text{ snow surface temperature}). \tag{12}$$

$$H_c + H_{sn} = (T_a - T_r)\rho c_p / r_a, \tag{13}$$

$$\lambda E_c = (e^*(T_c) - e_a)\rho c_p / \gamma / (W_c / \bar{r}_b + (1 - W_c) / (\bar{r}_c + \bar{r}_b)), \tag{14}$$

$$\lambda E_{sn} = (e^*((3)) - e_a)\rho c_p / \gamma / r_d, \tag{15}$$

$$\lambda E_c + \lambda E_{sn} = (e_a - e_r)\rho c_p / \gamma / r_a, \tag{16}$$

$$G_{pr} = (p_{sn} C_{v,sn}(T_{pr} - 273.15) + IF_0 C_{v,l}(T_{pr} - 273.15) + P_{sn} L_{li}, \tag{17}$$

where G_{pr} represents the enthalpy from rain falling or dry snow falling or the sum of them.

2.2 Governing equation of mass budget

Water storage in canopy

$$\frac{\partial M_c}{\partial t} = P_c - D_c - E_{wc} / \rho_w. \tag{18}$$

Snow water equivalent in snow layers:
For the surface layer $(j=3)$,

$$\frac{\partial (w_3 Dz_3)}{\partial t} = p_{sn} + IF_0 - IF_3 - RF_3 - E_{sn}. \tag{19}$$

For other layers $(j=2,1)$,

$$\frac{\partial (w_j Dz_j)}{\partial t} = IF_{j+1} - IF_j - RF_j. \tag{20}$$

Soil moisture in three soil layers:

$$\frac{\partial \theta_1}{\partial t} = \frac{1}{D_1}[Q_0 - Q_{1,2} - \frac{1}{\rho_w} E_{dc,1}], \tag{21}$$

$$\frac{\partial \theta_2}{\partial t} = \frac{1}{D_2}[Q_{1,2} - Q_{2,3} - \frac{1}{\rho_w} E_{dc,2}], \tag{22}$$

$$\frac{\partial \theta_3}{\partial t} = \frac{1}{D_3}[Q_{2,1} - Q_3 - \frac{1}{\rho_w} E_{dc,3}]. \tag{23}$$

Total runoff Q_r

$$RF_0 = P_{r,sn} - IF_0,$$
$$Q_r = RF_0 + Q_3 + RF_1 + RF_2 + RF_3, \tag{24}$$

where the fluxes, P_c, D_c, E_{wc}, IF_0, IF_j, RF_j, Q_0, $Q_{i,i+1}$, Q_3 and $E_{dc,i}$ are the functions of the atmospheric conditions, the predicted variables and the relevant resistances, and are

$$P_c = P(1 - e^{-K_c L_{tc}})V_c, \tag{25}$$

$$D_c = P_c \text{ if } M_c > S_c \text{ or } D_c = 0 \text{ if } M_c \leqslant S_c, \tag{26}$$

$$\lambda E_{wc} = (e^*(T_c) - e_a)\rho c_p / \gamma \cdot (W_c / \bar{r}_b), \tag{27}$$

$$P_0 = P - P_c + D_c, \tag{28}$$

$$P_{sn} = P_0, \text{ if } T_r < 272.15 \text{ or } = 0.0 \text{ if } T_r > 272.15 \tag{29}$$

$$P_{r,sn} = P_0, \text{ if } T_r > 272.15 \text{ or } = 0.0 \text{ if } T_r < 272.15 \tag{30}$$

$$IF_0 = \min(IF_{p3}, P_{r,sn}, avs_3), \tag{31}$$

$$IF_j = \min(IF_{p_{j-1}}, wf_j, avs_{j-1}), \tag{32}$$

$$IF_{p_{j-1}} = 4.2129 \times 10^5 \times d_{j-1}{}^2 \times \exp(-CE), \tag{33}$$

$$\lambda E_{dc} = (e^*(T_c) - e_a)\rho c_p / \gamma(1 - W_c)/(\bar{r}_c - \bar{r}_b). \tag{34}$$

λE_{dc} (partitioned into $\lambda E_{dc,1}$, $\lambda E_{dc,2}$ and $\lambda E_{dc,3}$), $Q_{i,i+1}$ and Q_3 are calculated based on formulas (46), (47), (53), (61) and (62) in Sellers et al. (1986).

All equations of (1), (8), (10), (18), (21)—(23) and relevant diagnostic equations come from original SSIB (SIB) (Sellers et al., 1986; Xue et al, 1991). As explained in the paper for the SIB (SSIB) model development, these equations did not consider the effects of snow and ice and some adjustment should be done. This adjustment for considering the effects of snow and ice on vegetation and soil zone has been completed by Sellers and his colleague in the APPENDIX B of the same paper and the adjustment has been completely followed in the new scheme. The APPENDIX B states "A preliminary attempt has been made to account for the effects of snow and ice within SIB. This currently consists of simple modifications to some of the parameters and calculations described in the rest of the paper. The various effects are itemized by processes below. (1) Definition of snow fall.······ (5) Energy partition. ······" (see APPENDIX B in Sellers et al., 1986). It has described the effects of snow falling and ice formation on interception, accumulation and evaporation of leaves, radiation transfer within canopy such as the scattering coefficients adjustments and the reflectance of the ground, energy release and absorption due to phase change of melting and freezing from snow to water and water to ice or vice versa on leaves and in soil and energy partitions and temperature adjustment, moisture movement, runoff and so on.

2.3 Rate of snow compaction and snow density change

Snow compaction processes include three components: destructive metamorphism, densification process due to snow load or overburden, and snow melting. In this subsection a brief description is presented only.

For the destructive stage, the empirical relation for compaction rate is used.

$$\left[\frac{1}{Dz_j}\frac{\partial Dz_j}{\partial t}\right]_m = -2.778 \times 10^6 \times C_3 \times C_4 \times \exp(-0.04(273.16 - T)). \tag{35}$$

For densification process at a slow rate, the compaction rate is a function of the pressure loading on a snow layer and can be expressed as

$$\left[\frac{1}{Dz_j}\frac{\partial Dz_j}{\partial t}\right]_w = -\frac{P_S}{\eta}, \tag{36}$$

where P_η is overburden weight loaded on a snow layer.

The total fractional compaction rate in the sub—layer, CR1, is the sum of the above two compaction rates.

$$CR_1 = \left[\frac{1}{Dz_j}\frac{\partial Dz_j}{\partial t}\right]_m + \left[\frac{1}{Dz_j}\frac{\partial Dz_j}{\partial t}\right]_w. \tag{37}$$

The rate of the snow density change ρ_s caused by the snow compaction is

$$\frac{d\rho_s}{\rho_s dt} = -CR1. \tag{38}$$

The meltwater generation, which does not change snow density, is also accompanied by a reduction of the sub—layer thickness. Its rate is estimated as

$$\left[\frac{1}{Dz_j}\frac{\partial Dz_j}{\partial t}\right]_{ml} = -\frac{dh_i}{h_i} = CR2, \tag{39}$$

where h_i is the dry snow mass in a unit depth and dh_i is the rate of dry snow mass melted in the unit depth. The total reduction rate for each layer is

$$\left[\frac{1}{Dz_j}\frac{\partial Dz_j}{\partial t}\right] = CR1 + CR2. \tag{40}$$

The detailed formulation and way to estimate or calculate parameters, C_3, C_4, P_S, η and others are given by Sun et al. (1999).

3. Solution of the governing equation

Preceding sections have presented the equations for the coupling system. It is very clear that all the variables and parameters in the system bear complicated interaction with each other, and in turn, an efficient numerical scheme is very essential to solve this system. The ideas used in SSIB and SAST, which employ explicit method for slow variables or implicit method for fast variables respectively to construct different differential equations (Sellers et al., 1986) are adapted for the interactive system. The corresponding procedures to solve the differential equations can be found in the papers (Sellers et al., 1986; Xue et al., 1991 and 1996; Sun et al., 1999) and are not discussed here again. However, since the way to describe the interaction between snow surface layer and vegetation in the new scheme is quite different from SSIB and SAST, the coupling equations to define the interaction of vegetation temperature and snow surface enthalpy are derived in sub—section 3.1. Then, by taking the advantage of the fact that the snow state can only be in either frozen or melting one, an efficient method without iteration, called as one test solver, is developed in sub—section 3.2 to solve this complicated system.

3.1. Combining equations of canopy temperatures and snow surface enthalpy

Referring to Fig. 1 and using similar idea described in Sellers et al. (1986), T_a and e_a can be eliminated from the equation system with all the resistance given, and two combining equations for the canopy temperature T_c and the snow surface enthalpy $H(3)$ can be derived. These two equations may then be solved by an implicit backward method.

Canopy temperature is given by

$$C_c\frac{\Delta T_c}{\Delta t} = R_{nc} + \frac{\partial R_{nc}}{\partial T_c}\Delta T_c + \frac{\partial R_{nc}}{\partial T}\Delta T(3) - H_c - \frac{\partial H_c}{\partial T_c}\Delta T_c - \frac{\partial H_c}{\partial T}\Delta T(3)$$

$$- \lambda E_c - \frac{\partial \lambda E_c}{\partial T_c}\Delta T_c - \frac{\partial \lambda E_c}{\partial T}\Delta T(3), \tag{41}$$

where $\Delta T_c = T_c^m - T_c^{m-1}$, $\Delta T(3) = T^m(3) - T^{m-1}(3)$ (m and $m-1$ indicate current and previous time steps).

Enthalpy of the snow surface layer

The differential equation (2) for this layer may be written as follows

$$\frac{\Delta H(3)}{\Delta t} = SH_{sn}(3) + Rn_{sn,L} - SH_{sn}(2) - H_{sn} - \lambda E_{sn} + G_{pr} - G_{sn}(z_2) \tag{42}$$

$$H(3) = C_v \times (T(3) - 273.16)f_i(3) \times L_{li} \times w_3 \times \rho_w, \tag{43}$$

where $\Delta H(3) = H(3)^m - H(3)^{m-1}$ and $SH_{sn}(2)$ is the solar radiation flux at the bottom of the surface layer.

$$G_{sn}(z_2) = (K(3) + K(2))(T(3) - T(2)) / (D_{z3} + D_{z2}) = (K(3) + K(2))T(3)$$
$$/ (D_{z3} + D_{z2}) - (K(3) + K(2))T(2) / (D_{z3} + D_{z2}) = C_{sn}T(3)C_{sn}T(2). \qquad (44)$$

As $Rn_{sn} = SH_{sn}(3) + R_{sn,L}$, Eq. (42) will become

$$\frac{\Delta H(3)}{\Delta t} = Rn_{sn} - SH_{sn}(2) - H_{sn} - \lambda E_{sn} + G_{pr} - C_{sn}T(3) - C_{sn}T(2). \qquad (45)$$

Then, the equation of the surface layer enthalpy similar to (41) is obtained

$$\frac{\Delta H(3)}{\Delta t} = Rn_{sn} + \frac{\partial Rn_{sn}}{\partial T_c}\Delta T_c + \frac{\partial Rn_{sn}}{\partial T}\Delta T(3) - H_{sn} - \frac{\partial H_{sn}}{\partial T_c}\Delta T_c - \frac{\partial H_{sn}}{\partial T}\Delta T(3)$$

$$- \mu E_{sn} - \frac{\partial \lambda E_{sn}}{\partial T_c}\Delta T_c - \frac{\partial \lambda E_{sn}}{\partial T}\Delta T(3) + G_{pr} - C_{sn}T(3) + C_{sn}T(2). \qquad (46)$$

Equation (46) becomes by using (43)

$$\frac{C_v \Delta T(3) - L_{li}w_3\rho_l\Delta f_i(3)}{\Delta t} = Rn_{sn} + \frac{\partial Rn_{sn}}{\partial T_c}\Delta T_c + \frac{\partial Rn_{sn}}{\partial T}\Delta T(3) - H_{sn} - \frac{\partial H_{sn}}{\partial T_c}T\Delta_c$$

$$- \frac{\partial H_{sn}}{\partial T}\Delta T(3) - \lambda E_{sn} - \frac{\partial \lambda E_{sn}}{\partial T_c}\Delta T_c - \frac{\partial \lambda E_{sn}}{\partial T}\Delta T(3)$$

$$+ G_{pr} - C_{sn}\Delta T(3) - C_{sn}(T^{m-1}(3) - T(2)), \qquad (47)$$

or

$$\frac{C_v \Delta T(3)}{\Delta t} = Rn_{sn} + \frac{\partial Rn_{sn}}{\partial T_c}\Delta T_c + \frac{\partial Rn_{sn}}{\partial T}\Delta T(3) - H_{sn} - \frac{\partial H_{sn}}{\partial T_c}\Delta T_c - \frac{\partial H_{sn}}{\partial T_{sn}}\Delta T(3)$$

$$- \lambda E_{sn} - \frac{\partial \lambda E_{sn}}{\partial T_c}\Delta T_c - \frac{\partial \lambda E_{sn}}{\partial T}\Delta T(3) + G_{pr} - C_{sn}\Delta T(3)$$

$$- C_{sn}(T^{m-1}(3) - T(2)) - L_{li}\rho_w(w_3 f_i^m(3) - w_3^{m-1}f_i^{m-1}(3)). \qquad (48)$$

Eqs. (41) and (48) are the final combining equations for obtaining the canopy temperature, snow surface temperature and dry snow fraction in snow surface layer, $f_i(3)$.

3.2 *Numerical scheme, especially for equations* (41) *and* (48)

In principle, the procedure and iteration way used in SSIB are followed in this scheme. It means that most of the variables with slow change are solved with explicit method. Two variables with fast change, that is the canopy temperature T_c and the snow surface temperature $T(n)$, are solved together with implicit backward difference equations just mentioned in subsection 3.1. Since two combined equations of (41) and (48) include three unknown variables $(T_c, T(3)$ and $f_i)$, one more constraint is needed to make the equations system well posed. The constraint comes from the actual surface snow state existence. There are three snow states in the real world: (a) completely frozen snow state when surface temperature is less than freezing point and the dry snow fraction $f_i = 1.0$; (b) the partly melted snow state when the temperature is equal to freezing point and $0.0 < f_i < 1.0$; and (c) completely melted snow state when the temperature is equal to freezing point and $f_i = 0$. This constraint helps us design a simple and efficient solver (called 'one step test method') to solve (41) and (48)
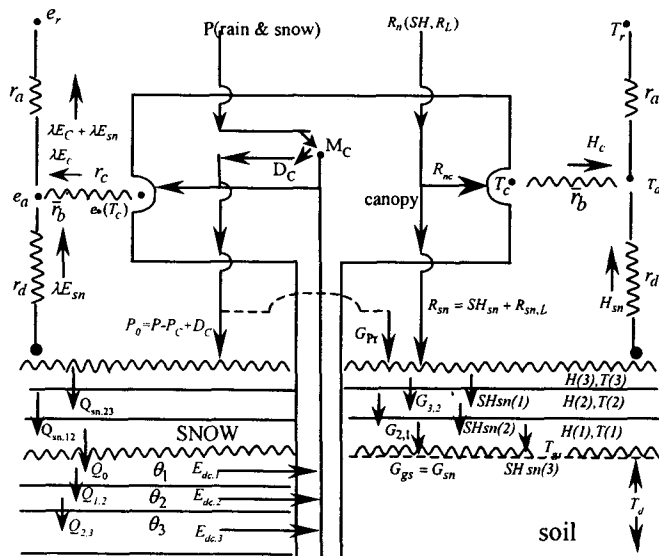
Fig. 1. Scheme of implementing SAST in SSIB.

in stead of using time consuming iteration scheme. The procedure of the one step test method consists of following steps

(i) At the beginning, it is tested by assuming that current state of the snow surface layer is in frozen state completely. It means that $f_i^m (n) = 1.0$, and then T_c^m, $T^m (n)$ will be solved from (41) and (48) directly. If the solution of $T^m (n)$ is less than 273.15, it means that the test is true and the solution is correct. If the solution of $T^m (n)$ is not less than 273.15,

(ii) then the surface layer will be definitely in either partially melted or completely melted state. In this case, one more test of assuming $T^m (n) = 273.15$ will be conducted, and then there is one solution for $f_i^m (3)$ from two possible solutions: a) if $0.0 < f_i^m (3) < 1.0$, the solution is true and the surface layer is in partial melting state, or b) if $f_i^m (n) < 0.0$, it means that the snow surface is melted completely and there is an extra input energy in addition to the part of energy used to melt the layer. In this case, the solutions should be $f_i^m (n) = 0.0$ and $T^m (n) = 273.15$, and the extra energy is transferred to the $(n-1)$ layer below. This procedure is applied to the numerical experiments in Section 4 successfully and saves computing time.

4. Numerical experiments using Russian and French snow data

The French data and part of the Russian data sets are used to test the new scheme. French data were obtained for 1989, 1993–1994 and 1995 at one station with short grass cover. The atmospheric conditions driving the model were obtained from observations. Russian data from six stations, located from 48°N to 58°N and from 40°E to 135°E, are selected from 130 Russian stations (Robock et al., 1995). The observational sites at each of the stations are relatively flat also with short grass cover. The meteorological and actinometric data used to force the models were observed every 3 hours for a six–year period (1978 through 1983).

More detailed information regarding this data set and its application can be found in Robock et al. (1995).

Figures 2a–2b, 3a–3b and 4a–4b show comparisons between simulation results (using o or +) of the new scheme and the observational data (using symbol •) for snow depth and surface temperature for the years 1995, 1993–1994 and 1989 in Col de Porte (45°N, 6°E). The vegetation of grass type in SSIB is used for this station. For the surface temperature of 1995 and 1993–1994 and the snow depth of 1995, 1993–1994 and 1989, the model results are close to the observational data in either trends or values. There are some differences between predicted temperature and measured one. One occurs when snow surface is in melting situation but whole snow pack still exists. The difference is that the predicted temperature is always equal to 273.15 and measured one may exceed 273.15. This difference may come from the error of measured data explanation because snow surface layer temperature must be equal to 273.15 and temperature of entire snow pack should not exceed freezing temperature (273.15) when only snow cover surface starts to melt and snow cover still exists. Another one is shown in Figs. 3b and 4b and occurs after each May. It may come from the SSIB run itself because the snow cover has disappeared already at that time and only original SSIB works after each May.

There is only one observational datum for runoff in 1995. Figure 2c shows the comparison between simulation result (with symbol o) and the observational data (with symbol •). In this simulation, the soil type under snow cover is considered as fine soil. The result for the simulation agrees with the observation very well. We also use coarse (i.e. sandy) soil for simulation, and the result for the simulation is in poor agreement with the observation. It indicates that, in order to accurately predict seasonal snow cover behavior, the realistic description of physical properties of underlying surface, frozen soil, is very important. This finding is consistent with the Xue's results for the Russian data simulation (Xue et al., 1996).
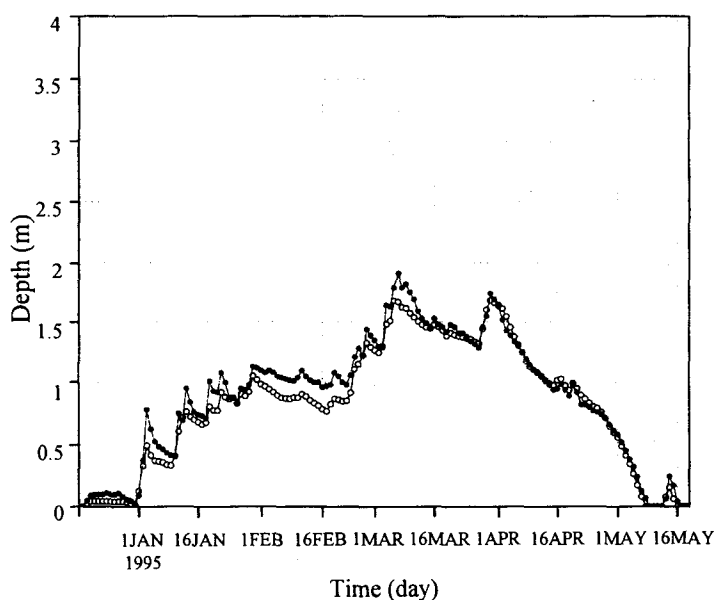

Fig. 2a. Daily average snowdepth at Col de Porte, France. o simulation; • observation
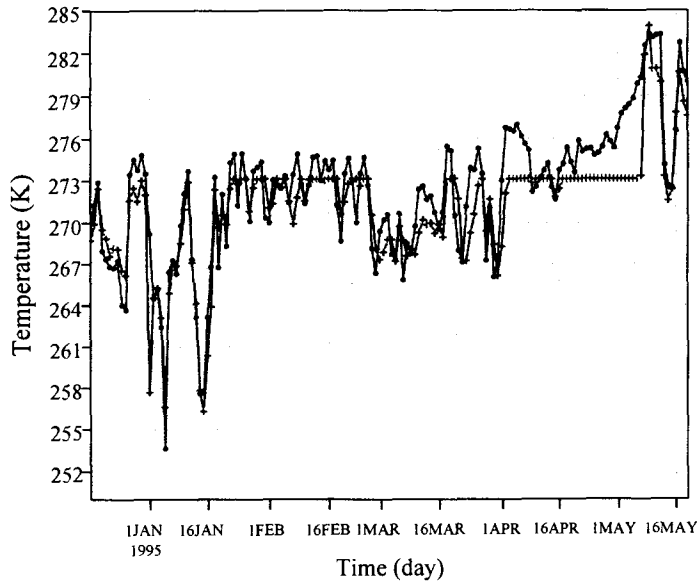
Fig. 2b. Daily average surface temperature at Col de Porte, France. + simulation; ● observation
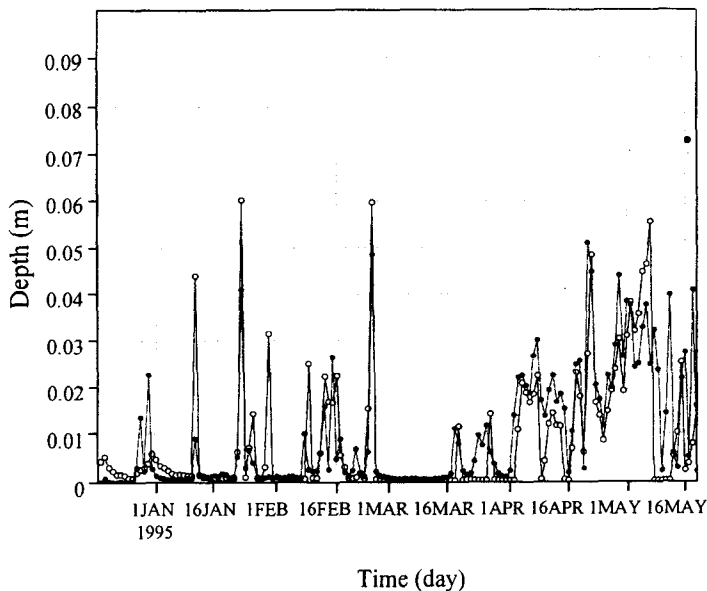

Fig. 2c. Daily average runoff depth Col de Porte, France. o simulation; ● observation

Using the part of Russian data, the model is integrated for six years. Figures 5a—5c to 6a—6c show the comparison between model simulation and the observations for snow depth, snow water equivalent and snow surface temperature in Kostroma (51.4°N, 48.3°E) and Yershov (57.8°N, 40.9°E). The same vegetation type (grass type in SSIB) is used for the two stations. For station Kostroma, the figures indicate that the simulations are generally in good
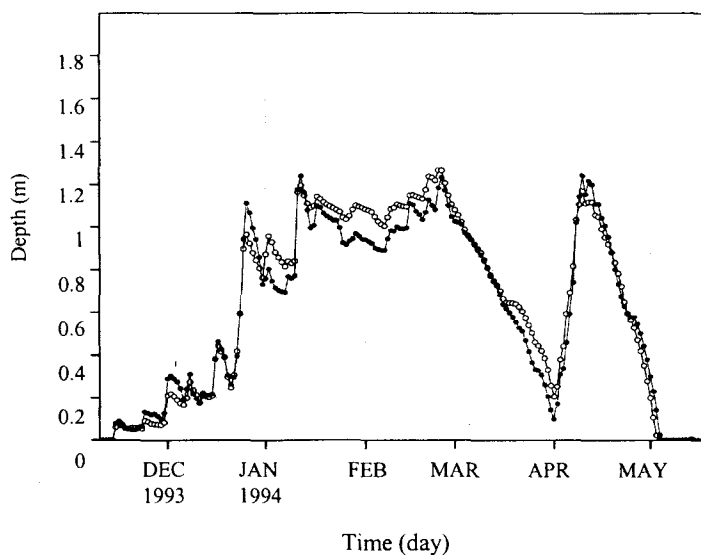
Fig. 3a. Daily average snow depth at Col de Porte, France. o simulation; ● observation
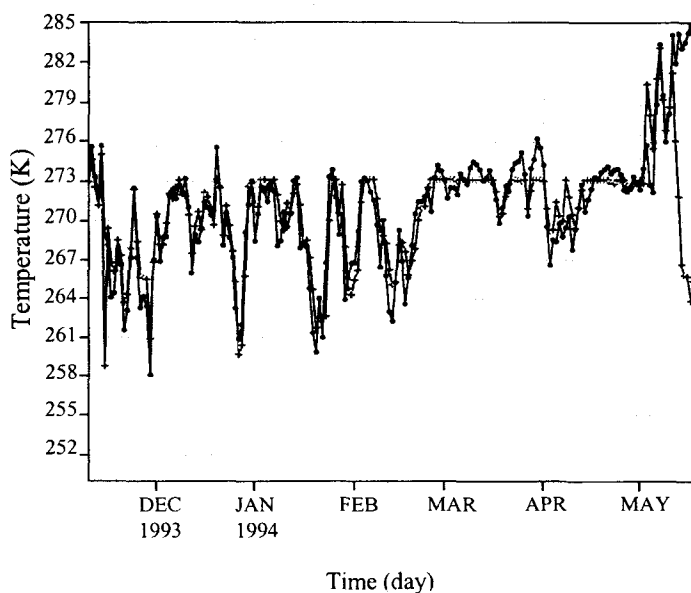

Fig. 3b. Daily average snow surface temperature at Col de Porte, France.+ simulation; ● observation

agreement with the observations for snow depth, snow water equivalent and surface tempera-
ture, especially during the winter accumulation season. For station Yershov, Fig. 6c shows
the comparison of predicted surface temperature with observational data. The result indicates
that there is good agreement in trend and better agreement in value. However, from Figs.
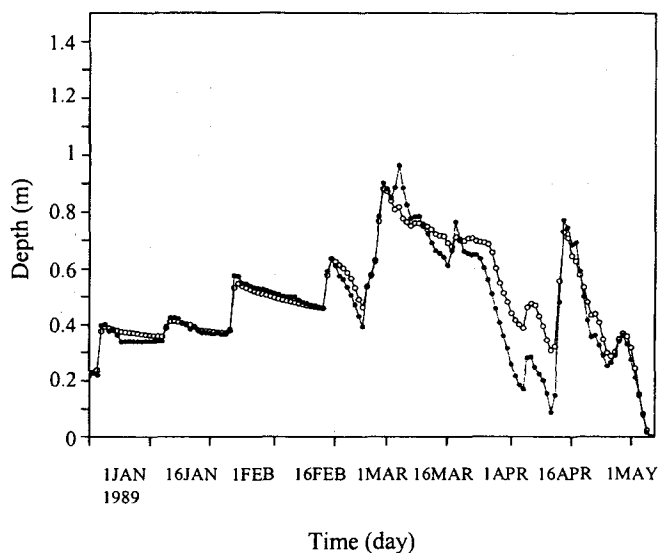6a—6b at Yershov, there is certain discrepancy in results of snow depth and snow water

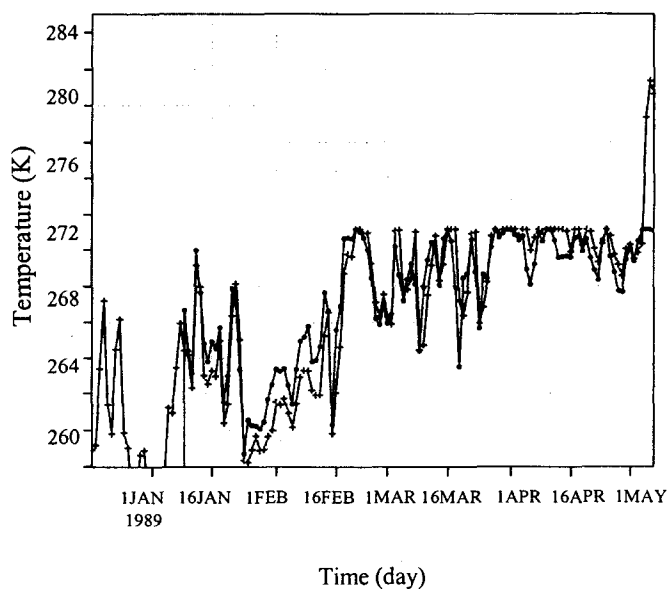Fig. 4a. Daily average snow depth at Col de Porte, France. o simulation; ● observation

Fig. 4b. Daily average snow surface temperature at Col de Porte, France. + simulation; ● observation

equivalent between modeling and observation. The snow thickness for Kostroma was from 50 cm to 1 m, and the thickness for Yershov was less than 5 cm for most time period in six years and the greatest thickness of snow pack was only 0.12 m but only occurred in a short time period in 1978. It suggests that the scheme of SSIB implemented with SAST can work well on thick snow pack but not well on thin snow cover. The suggestion has been well attested by the
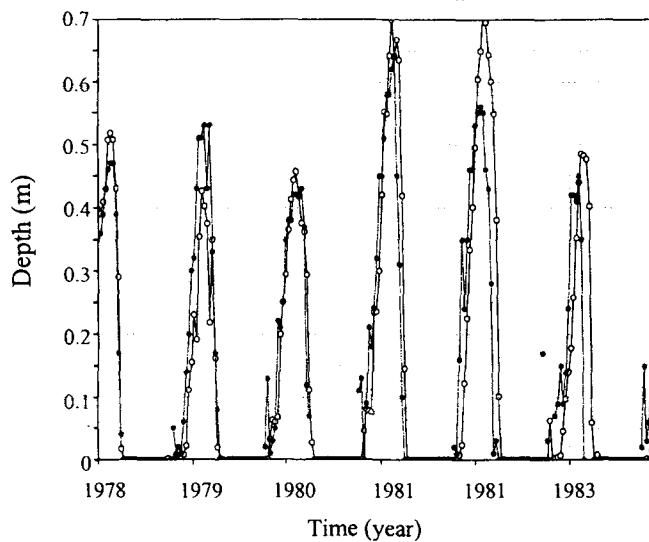
Fig. 5a. Daily average snow depth at Kostroma. o simulation; • observation

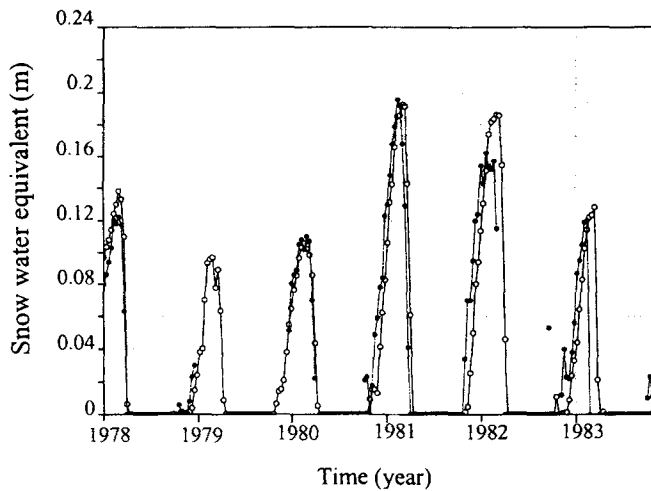Fig. 5b. Daily average snow water equivalent at Kostroma. o simulation; • observation
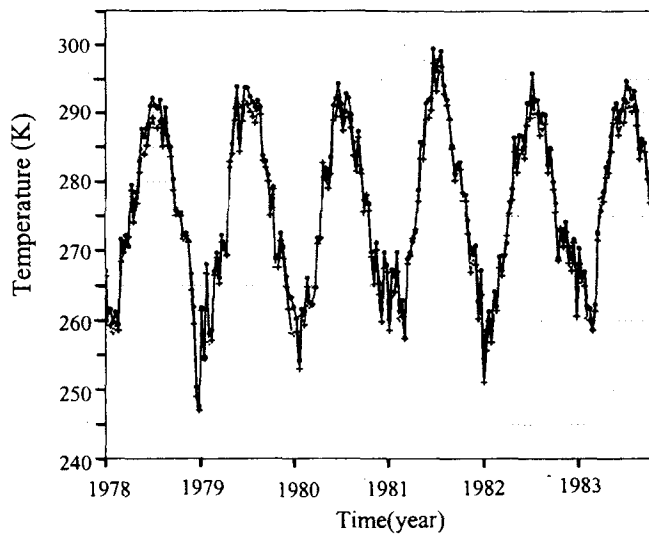

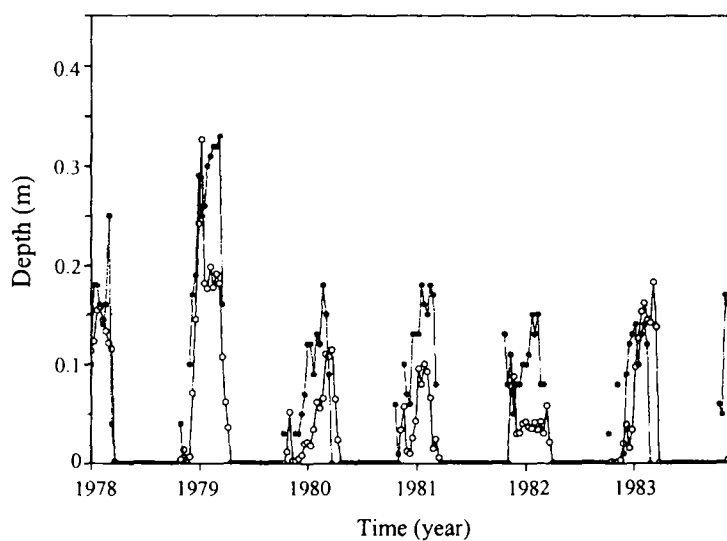Fig. 5c. Daily average snow surface temperautre at Kostroma. + simulation; • observation

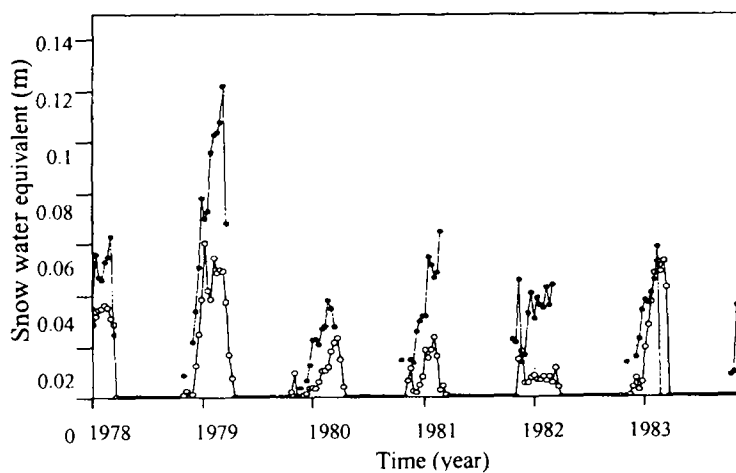Fig. 6a. Daily average snow depth at Yershov. o simulation; ● observation

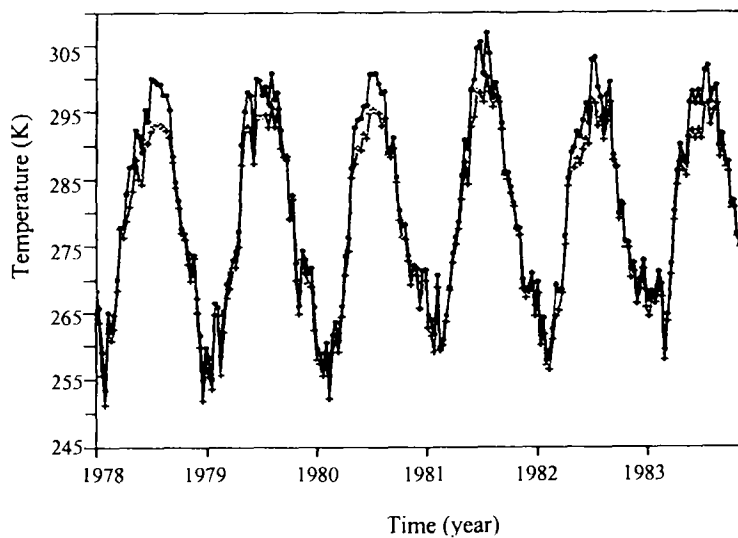Fig. 6b. Daily average snow water equivalent at Yershov. o simulation; ● observation

Fig. 6c. Daily average snow surface temperature at Yershov. + simulation; ● observation

modeling results much closer to the measured data in France (all measured snow cover thickness is more than 1 m) discussed above. The exact cause of worse function on thin snow cover has not been understood completely, however, several important factors should be pointed out next which may give explanation for the discrepancy to some degree. 1) Some factors, for example, such as snow drifting, are not considered in the model, and they may contribute to this discrepancy. 2) As we mentioned before, there is a switch in the new scheme, and the new scheme of implementing SAST in SSIB will be applied only after snow pack depth exceeds 0.05 m. It means that the modeling simulation at Yershov is mainly controlled by original SSIB version for most operational time period and the shortage of worse result agreement between modeling and observation at Yershov may come out from SSIB itself. 3) The quality of Russian data for driving model and for model evaluation purpose may not be so reliable to some degree and it will affect the comparison reality.

In general, this paper has presented the new scheme which sandwiches SAST model with physically based description between vegetation and soil body and in turn may improve the original SSIB function. By using the efficient one test solver, the complicated system can be solved very well. Based on the observational data from Russia and France, the new scheme has been tested successfully and results show its potential application in climate and hydrology studies. However, due to the complexity of snow physics, more data to thoroughly validate the scheme are necessary, in particular for the key parameterizations of melted water flow, thermal heat conductivity, and turbulence transfer. Snow surface albedo is a very important factor. However, there are only some data sets from snow cover exposed over bare soil and few albedo data of snow cover under vegetation that can be used to verify the scheme of radiation transfer within canopy and interaction between canopy and snow cover underneath. As mentioned before, the interaction of soil zone with snow cover is also very important, and there is also lack of complete data sets in snow—soil continuum for modeling study. Anyway, more and more observational data obtained in this aspect are necessary and critical to further improve the understanding of air—vegetation—snow—soil interactions.

APPENDIX

C_{gs}, C_d	Effective heat capacities for soil surface and deep soil layer
C_c, C_v	Heat capacity of canopy layer and average volumetric heat capacity of snow
$C_{v,sn}, C_{v,l}$	Specific heat capacities of ice and liquid water
CE	A parameter.
D_c	Water drainage rate from canopy
D_i, Dz_j	Thickness of ith soil layer and jth snow layer
E_{wc}	Rate of evaporation of water from the wet portion of the leaves
E_c, E_{sn}	Evapotranspiration rate from canopy and snow surface
E_{sn}	Evaporation rate at the snow surface and positive upward
$E_{dc,i}$	Abstraction rate of soil moisture by canopy transpiration from ith layer
G_{sn}	Heat flux through the snow layers

G_{gs}	Heat flux into soil surface, which equals G_{sn} at snow bottom
G_{pr}	Heat energy brought to snow surface layer by precipitation
$G_{pr} = Z,t,\tau$	Vertical coordinate (m), time (s), and the day length ($=86400$ s)
$H(z)$	Enthalpy of snow body at depth Z
H_c, H_{sn}	Sensible heat from the canopy and snow surface
IF_0	Rainfall contribution to the liquid water infiltration flux at the snow surface (m / s)
IF_j	Water infiltration flux at the interface between jth and (j+1)th snow layer
$K(j)$	Effictive heat conductivity of snow in jth layer
K_s	Hydraulic conductivity of saturated soil
K_c, L_{tc}, V_c	Extinction coefficient of leaves, leaf area index and vegetation coverage
L_{iv}, L_{lv}, L_{li}	Specific latent heats from ice to vapour, water to vapour or water to ice
M_c	Water stored on leaves
P	Precipitation rate above the canopy ($= P_{r,sn} + P_{sn}$)
$P_{r,sn}$	Rain fall rate
P_{sn}	Rate of dry snow fall which piles up on the snow surface layer
P_c	Interception rate of precipitation by canopy
P_0	Effective precipitation rate on snow surface
Q_0	Infiltration rate of melted water into soil surface ($= \min.(wf_3, K_S)$)
$Q_{i,i+1}$	Flow rate between layers i and $i+1$
Q_3	Gravitational drainage out off soil layer 3
RF_j	Runoff from the bottom of layer j
Rn_c	Absorbed net radiation by the canopy
$Rn_{sn,L}$	Net long wave radiation absorbed by the snow surface
$SH_{sn}(Z)$	Beam radiation flux through the snow body
SH_{sn}^*	Beam radiation flux reached the snow surface
S_c	Maximum value of water stored on leaves
T_r, e_r	Air temperature and vapor pressure at reference height
T_a, e_a	Air temperature and vapor pressure within canopy
T_c, $T(z)$	Tempertures of canopy and snow layer at Z
T_{gs}, T_d	Tempertures of ground surface and deep soil layer
T_{pr}	Precipitation temperature
W_c	Fraction of wet leaf area
Z,t,τ	Vertical coordinate (m), time(s), and the day length($=86400$ s)
avs_{j-1}	Available water storage space in snow layer ($j-1$)
$e^*(T_a), e^*(T(z))$	Saturated vapour pressures at the temperature, T_a and $T(z)$
$f_i(j), f_l(j)$	Mass fractions of ice and liquid water of jth layer in snow body
$\bar{r}_b, \bar{r}_c, r_d, r_a$	Average boundary layer and canopy resistances, aerodynamical resistance
wf_j	Drainage rate form the bottom of snow layer j($= IF_j + RF_j$)
w_j	Volumetric snow water equivalent in sub–layer j with thickness Dz_j
α	Albedo of snow surface
κ	Snow extinction coefficient to short– wave radiation
ρ, T_r, e_r, C_p	Density, temperature, vapor pressure and specific heat capacity of air

ρ_w	Liquid water density
λ	Specific latent heat from ice to vapour
γ	Psychrometric constant
θ_i	Volumetric soil moisture in soil layer i
θ_s	Soil moisture at saturation
γ_{j-1}, d_{j-1}	Bulk density of dry snow and snow grain size in layer ($j-1$)

The method to estimate some of the parameters above can be found in the papers (Sellers et al., 1986; Xue et al., 1991, 1996; Sun et al., 1999).

REFERENCES

Anderson, E.A., 1976: A point energy and mass balance model of a snow cover. *NOAA Technical Report NWS*, 19, Office of Hydrology. National Weather Service, Silver Spring, MD, 150pp.

Barnett, T.P., L. Dumenil, U. Schlese, E. Roeckner, and M. Latif, 1989: The effect of Eurasian snow cover on regional and global climate variations. *Journal of Atmospheric Science*, 46, 661—685.

Cohen, J., and D. Rind, 1991: The effect of snow cover on the climate. *Journal of Climate*, 4, 689—706.

Jordan, R., 1991: A one—dimensional Temperature Model for a Snow Cover. *CRREL*, Special Report, 91—1b, 49pp.

Kukla, G., 1981: Climate role of snow cover, in Allison, A (ed.). *Sea Level, Ice and Climatic Change*, International Association of Hydrological Sciences Publication, Washington DC, 131, 79—107.

Loth, B., and H.F. Graf, 1992: Snow cover model for global climate simulation. *Journal of Geophysical Research*, 98(D6), 10451—10464.

Lynch—Stieglitz, M., 1994: The development and validation of a simple snow model for the GISS GCM. *Journal of Climate*, 7, 1842—1855.

Robock, A., K.V. Vinnikov, C.A. Schlosser, N.A. Speranskaya, and Y. Xue, 1995: Use of Russian soil moisture and meteorological observations to validate soil moisture simulations with biosphere and bucket models. *Journal of Climate*, 8, 15—35.

Sellers, P.J., Y. Mintz, Y.C. Sud., and A. Dalcher, 1986: A Simple Biosphere Model(SIB) for Use within General Circulation Model. *Journal of Atmospheric Science*. 43, 505—531.

Slater, A.G., A.J. Pitman and C.E. Desborough, 1998: The validation of a snow parameterization designed for use in general circulation models. *International Journal of Climatology*, 18, 595—617.

Sun, S.F., J. Jin, and Y. K. Xue, 1999: A simple snow—atmosphere—soil transfer model. *Journal of Geophysical Research*, 104(D16), 19587—19597.

Vernekar, A.D., J. Zhou, and J. Shukla, 1995: The effect of Eurasian snow cover on the Indian monsoon. *Journal of Climate*, 8, 248—266.

Walsh, J. E., W.H. Jasperson and B. Ross, 1985: Influence of snow cover and soil moisture on monthly air temperature. *Monthly Weather Review*, 113, 756—768.

Wiliams, J., 1975: The influences of snow cover on the atmospheric circulation and its role in climate change: an analysis based on results from the NCAR global circulation model. *Journal of Applied Meteorology*, 14, 137—152.

Xue, Y., P. J. Sellers, J.L. Kinter III, and J. Shukla, 1991: A Simplified Biosphere Model for Global Climate Studies. *Journal of Climate*, 4, 345—364.

Xue, Y., F. J. Zeng, and C.A. Schlosser, 1996: SSIB and its sensitivity to soil properties—a case study using HAPEX—Mobilhy data. *Global & Planetary Change*, 13, 183—194.

在简化的简单生物圈模式中结合新的雪盖模型

孙菽芬　　薛永康

摘　　要

本文提出了将一个新的雪盖模型(SAST)与简化的简单生物圈模型(SSIB)相结合后的 SSIB 模型的改进形式,并利用俄罗斯及法国的观测数据对改进后的模型进行了检验. 文中描述了改进后的 SSIB 模型中空气-植被-雪盖-土壤复杂系统之间有关能量和质量交换的过程,并给出为求解这一组非线性方程组所发展的有效计算方法. 利用俄罗斯及法国的观测结果对这一新的改进模型功能进行了验证. 结果表明改进后 SSIB 的数值模拟结果能较好地重现现场观测数据,说明这个新的改进形式可以推广用于气候研究.

关键词: 雪盖模型(SSAT), SSIB, 结合, 检验